

4. EXPERIMENTAL PROCEDURE

The sinter pot test was designed according to the requirements of real plant conditions. The sinter pot test can be conducted for several different purposes but the main aim is to evaluate the influence of different sinter mixture compositions on the quality of the sinter product. The results of the sinter pot test can also be used for sinter process optimisation. From the results of the sinter pot tests, the sintering behaviour of the raw materials in the sinter mixture are determined, typical quality measures being production rate, fuel consumption rate and sinter quality.

Representative samples of the different raw materials used in the sinter plant were obtained and prepared for sinter pot tests. The percentages of the different raw materials used in the sinter mixture are given in **Table 2**. The sinter mixture was composed in order to obtain a sinter with a FeO content of seven percent and basicity (CaO/SiO₂) of two. The sinter mixture and amount of water added were composed to achieve similar bed permeabilities. The dry raw materials were mixed together in a rotary mixer. The water was added and further mixing for six minutes resulted in adequate granulation.

Table 2: Sinter mixture

	Series 1 [mass %]	Series 2 [mass %]
Pressure drop	1100mmH ₂ O	1500mmH ₂ O
Iron ore A	14.60	14.43
Iron ore B	18.77	18.55
Iron ore C	9.38	9.26
Return fines	28.83	28.61
Lime	2.68	3.62
Quick lime	1.99	1.99
Dolomite	5.10	4.89
Coke	3.23	3.23
Waste material mixture	9.79	9.79
Water	5.47	5.47
CaCl ₂	0.16	0.16

The sinter pot was prepared with a grid layer consisting of -40+20mm sinter particles. The grid layer was 50mm in height. The raw materials were fed from the rotary mixer

into the sinter pot with a conveyer system. The total bed height was 500mm. The surface of the mixture was ignited with a gas flame under a pressure drop of 500mm H₂O over the bed. The ignition temperature measured on the surface of the sinter bed was 1000°C. After an ignition time of 1.5 minutes the gas flame was stopped and the pressure drop over the sinter bed was increased. **Figure 3** and **Figure 4** are schematic diagrams showing the sinter pot test equipment and set-up. In these tests the pressure drop over the sinter bed was controlled to a nearly constant value. Measurement of the off-gas volumes was done at the outlet of the sinter pot. No correction for volume increase due to water vapour and CO₂ formation was done.

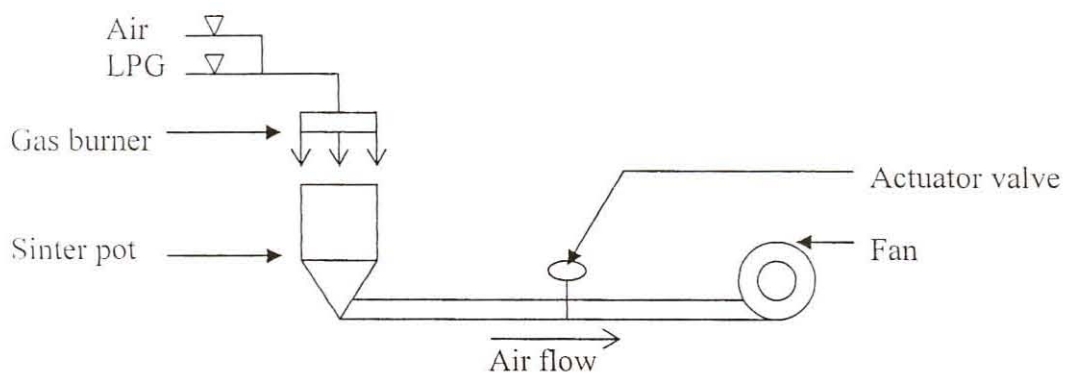


Figure 3: Sinter pot test equipment

In the first series of sinter pot tests the pressure drop was increased to 1100mm H₂O after ignition. The sintering cycle ended when the off-gas temperature reached a maximum temperature and started to decline. In the cooling cycle the sinter was cooled in the sinter pot under a pressure drop of 1100mm H₂O over the sinter bed. The cooling cycle ended when the off-gas temperature reached 150°C. In order to increase the airflow rate through the sinter bed during sintering the pressure drop over the sinter bed was increased to 1500mm H₂O after ignition during the second series of sinter pot tests. The sintering cycle ended when the off-gas temperature reached a maximum temperature and started to decline. In the cooling cycle the sinter was cooled in the sinter pot under a pressure drop of 1500mm H₂O over the sinter bed. The cooling cycle again ended when the off-gas temperature reached 150°C.

Process parameters were recorded during the sinter pot tests in order to characterise the sinter pot test conditions of each series. The temperature profile at different heights in the sinter bed was determined with thermocouples (**Figure 4**) to represent the temperature profile in the top layer, middle layer and bottom layer of the sinter pot. These K-type thermocouples were inserted into the sinter bed before the sinter was ignited by the gas flame.

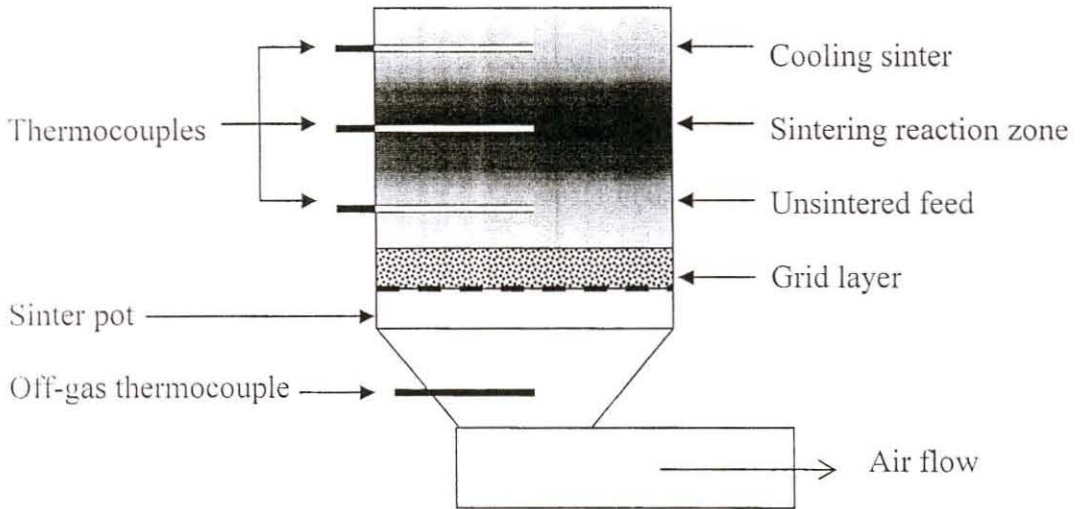


Figure 4: The sinter pot with thermocouples

Three sinter pot tests were performed in each series according to the sinter pot test standard procedure. Each sinter cake obtained from the sinter pot tests was physically divided into three layers to form a top layer, middle layer and bottom layer. The sinter from each layer was combined to produce a representative sample of each layer. The different layers of both series were separately prepared for evaluation. The aim was to characterise the properties of the sinter in the top layer, middle layer and bottom layer of each series.

The sinter was prepared according to a procedure to represent the preparation stage of sinter at the sinter plant. The preparation procedure also ensures that the samples taken from the sinter are representative of the sinter produced in the sinter pot test. Therefore, the different samples represent the sinter in the top layer, the sinter in the middle layer and the sinter in the bottom layer of each series.

A sieve analysis was conducted on each sample. Material representative of the size fraction $-40+10\text{mm}$ was prepared for the tumbler test (ISO3271). The tumbler test (ISO3271) was used to determine the physical properties i.e. the strength of the sinter in each sample. Material representative of the size fraction $-25+16\text{mm}$ was prepared for chemical and phase analyses.

5. RESULTS AND DISCUSSION

5.1 PRESSURE DROP AND AIRFLOW RATE

In the first series of sinter pot tests the pressure drop over the sinter bed was increased to $1100\text{mm H}_2\text{O}$ after the ignition sequence (**Figure 5**). The airflow rate through the sinter bed increased due to the applied pressure drop of $1100\text{mm H}_2\text{O}$ (**Figure 6**). During the sintering cycle the permeability of the bed decreased due to the sintering reactions that were taking place and formation of the melt⁽⁵⁾. As a result, the airflow rate decreased to a minimum of 2115 l/minute after 17 minutes. The permeability of the sinter bed improved due to the solidification of the phases resulting in the airflow rate to increase again towards the end of the sintering cycle. The average airflow rate during the sintering cycle was 2983 l/minute .

The sintering cycle ended when the off-gas temperature reached a maximum temperature of 417°C after 21 minutes and started to decline (**Figure 7**). The off-gas temperature increases because the combustion layer moves downwards in the sinter bed and the remaining raw materials mixture does not cool the off-gas any more. The airflow rate at the end of the sintering cycle is almost the same as at the start of the sintering cycle.

In the cooling cycle the sinter was cooled in the sinter pot under a pressure drop of $1100\text{mm H}_2\text{O}$ over the sinter bed. The resulting airflow rate is very high due to the microstructure of the sinter which has good permeability. The cooling cycle ended when the off-gas temperature reached 150°C .

Figure 5: Pressure drop during the sinter pot tests

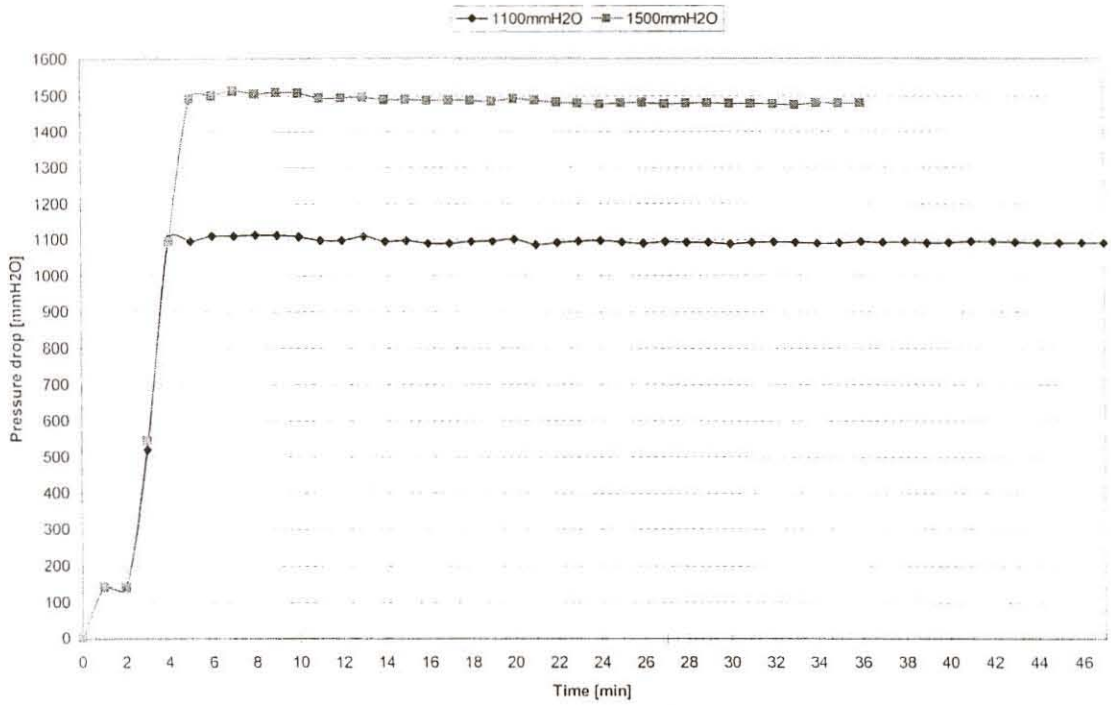


Figure 6: Air flow rate during the sinter pot tests

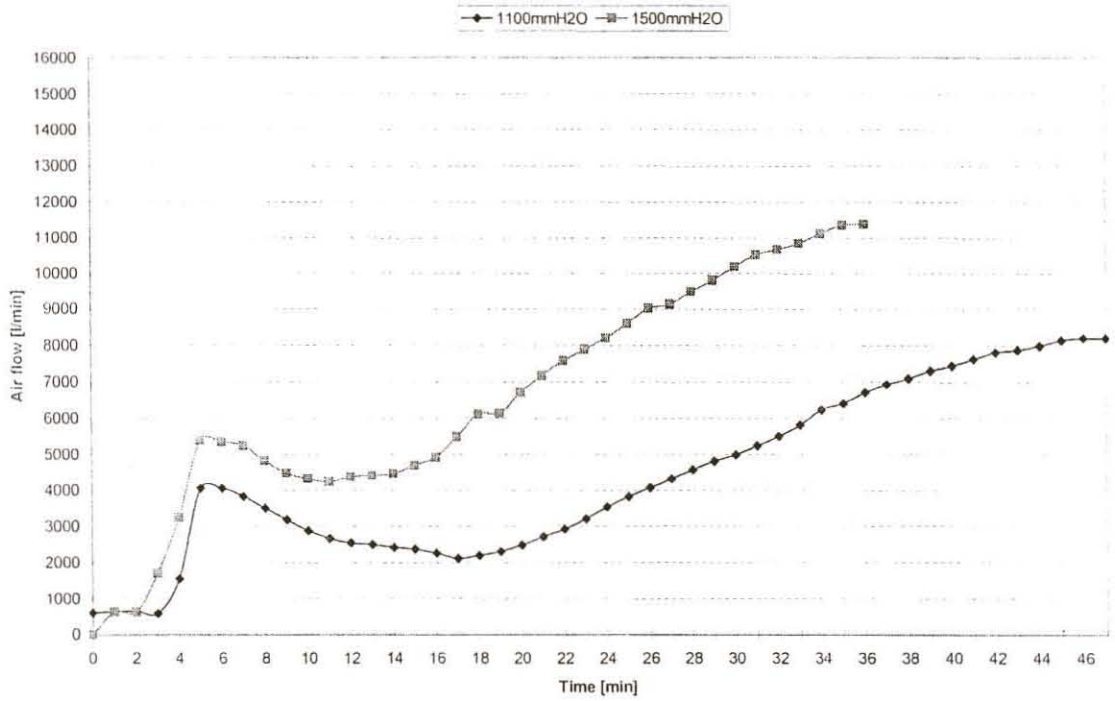
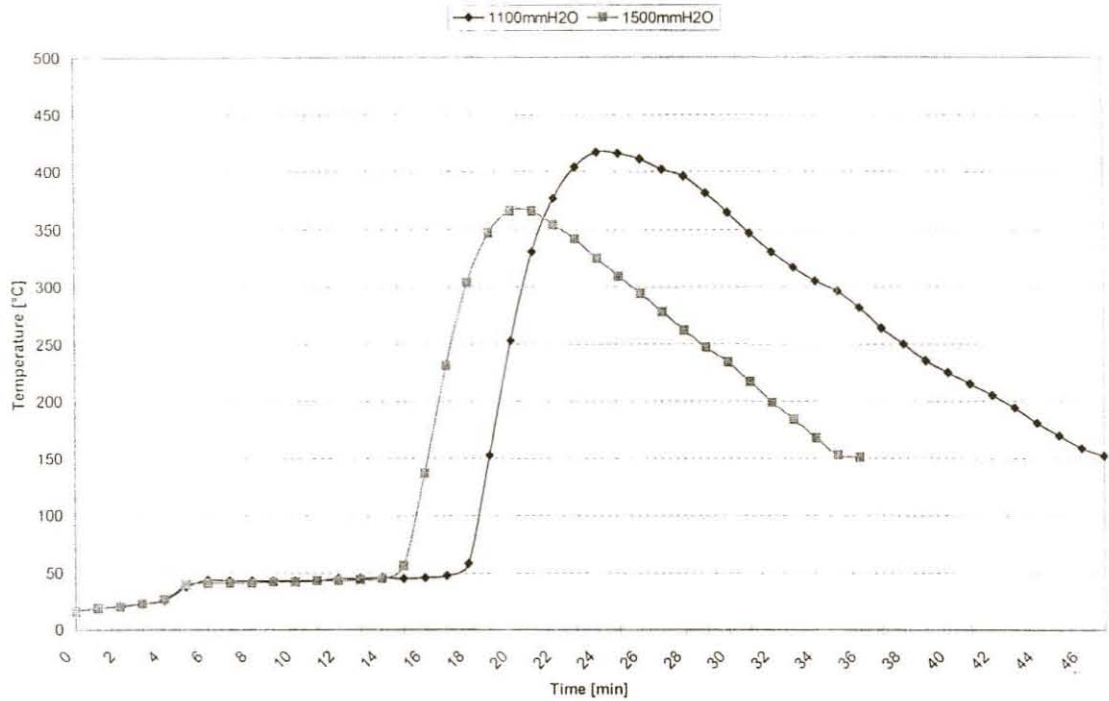


Figure 7: Off-gas temperature during the sinter pot tests



In order to increase the airflow rate through the sinter bed during sintering the pressure drop over the sinter bed was increased to 1500mm H₂O during the second series of sinter pot tests (**Figure 5**). **Figure 6** shows the resulting airflow rate. The airflow rate through the sinter bed increased due to the applied pressure drop of 1500mm H₂O (**Figure 6**). During the sintering cycle the permeability of the bed decreased due to the sintering reactions that were taking place and formation of the melt. As a result, the airflow rate decreased to a minimum of 4237 l/minute after 11 minutes. The permeability of the sinter bed improved due to the formation of sinter resulting in the airflow rate to increase again towards the end of the sintering cycle.

The sintering cycle ended when the off-gas temperature reached a maximum temperature of 366°C after 16 minutes and started to decline (**Figure 7**). The off-gas temperature increases because the combustion layer moves downwards in the sinter bed and the remaining raw materials mixture does not cool the off-gas any more. The airflow rate at the end of the sintering cycle is almost the same as at the start of the sintering cycle.

It is important to note that the airflow rate in the sintering and cooling cycle of series two (1500mm H₂O) was higher than the airflow rate in series one (1100mm H₂O). The increased pressure drop over the sinter bed in series two resulted in the faster downward movement of the reaction zone and therefore a shorter sintering time. Therefore, it is possible to increase the airflow rate and to decrease the sintering time by increasing the pressure drop over the sinter bed. Some of the more important results of both series are summarised in **Table 3**.

Table 3: Pressure drop and airflow rate characteristics of sintering and cooling cycle during Series 1 and Series 2

		Series 1	Series 2
Sintering cycle			
Pressure drop over sinter bed	mmH ₂ O	1100	1500
Airflow after ignition sequence	l/minute	4062	5389
Minimum airflow	l/minute	2115	4237
Airflow at end of sintering cycle	l/minute	4069	7174
Average airflow rate	l/minute	2983	5194
Duration of sintering cycle	minutes	21	16
Maximum off-gas temperature	°C	417	366
Cooling cycle			
Pressure drop over sinter bed	mmH ₂ O	1100	1500
Average airflow rate	l/minute	6629	9723
Duration of cooling cycle	minutes	21	15

5.2 TEMPERATURE-TIME-CHARACTERISTICS

The temperature profile at different heights in the sinter bed was determined with thermocouples to represent the temperature profile in the top layer, middle layer and bottom layer of the sinter pot. The temperature profile at 1100mm H₂O is shown in **Figure 8** while the temperature profile at 1500mm H₂O is shown in **Figure 9**.

The temperature-time-characteristics in each layer are summarised in **Table 4**. Heating rates were determined from a straight line tangential to the temperature curve at 700°C. The heating rates in series two with the higher pressure drop over the sinter bed (1500mm H₂O) exceeded the heating rates of series one with the lower pressure drop over the sinter bed (1100mm H₂O).

Figure 8: Temperature profile at 1100mmH₂O

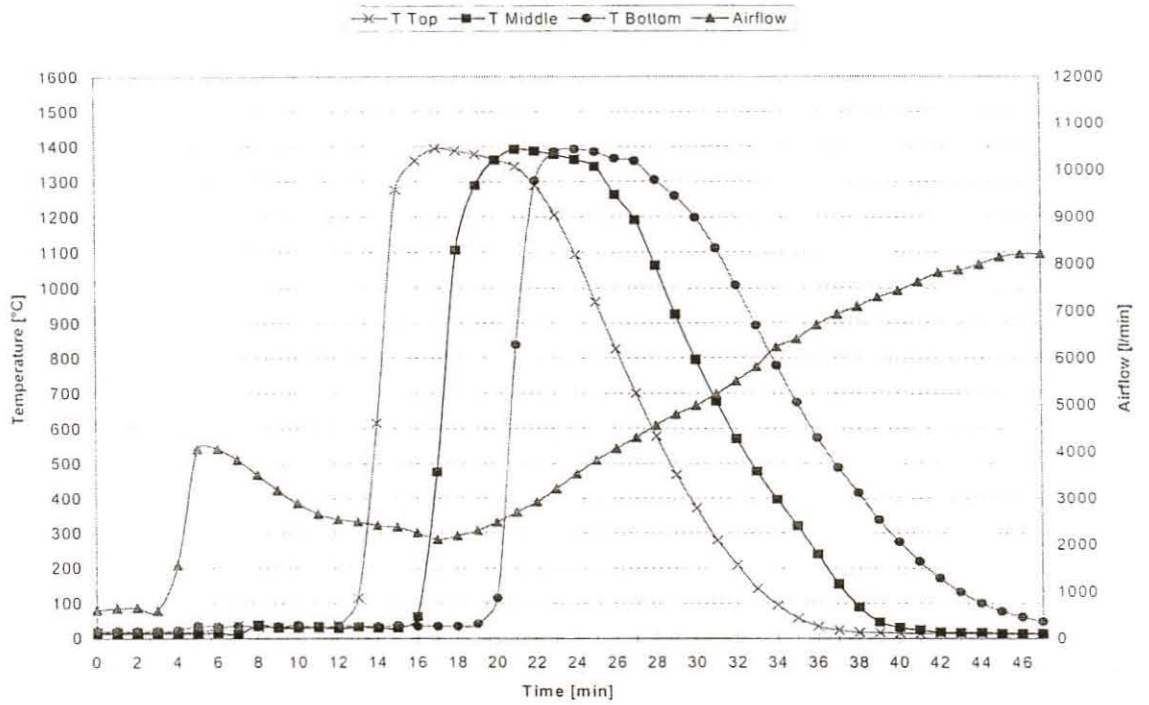
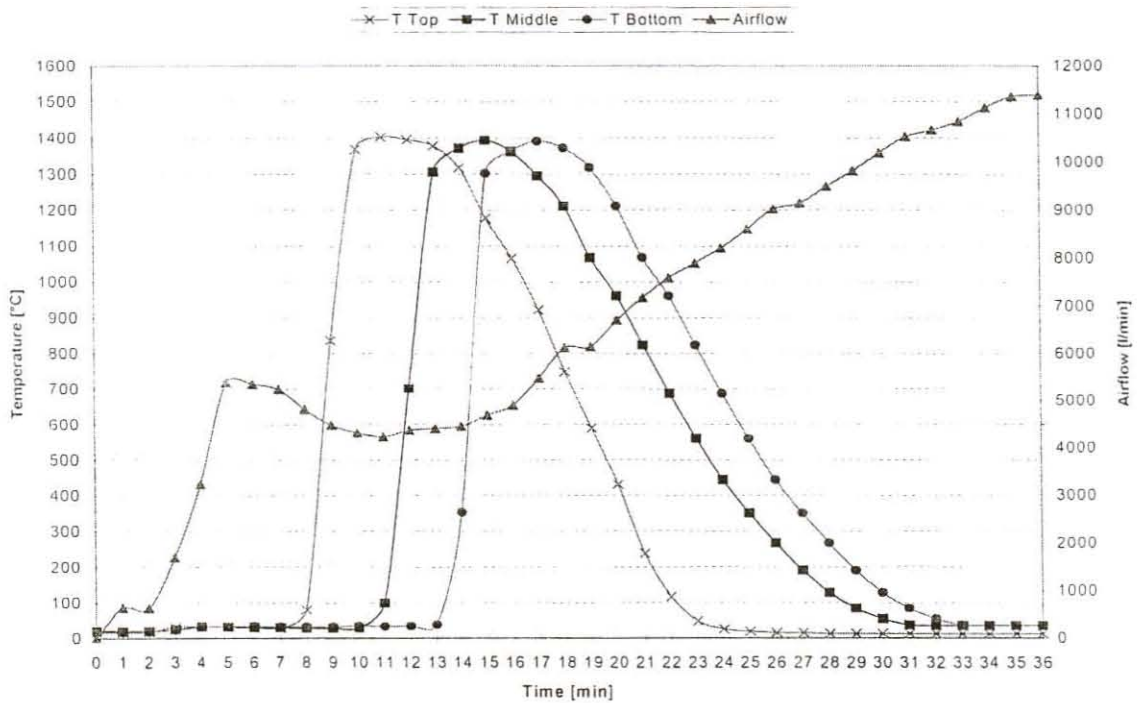


Figure 9: Temperature profile at 1500mmH₂O



The highest heating rate in both series was found to be in the bottom layer. Reported heating rates are between 700°C/min and 1000°C/min⁽¹³⁾. The maximum temperatures reached in each layer in both series did not differ as much. This is possibly due to the high coke consumption during the sinter pot tests in both series.

Table 4: Temperature-time-characteristics

Parameter	Top	Middle	Bottom
Series 1: 1100mm H₂O			
Heating rate [°C/min]	641	641	751.9
T maximum [°C]	1393	1391	1391
Cooling rate [°C/min]	125	112.5	102.2
Time at T>1100°C [min]	9.3	9.8	9.6
Series 2: 1500mm H₂O			
Heating rate [°C/min]	751.9	641	1123.6
T maximum [°C]	1402	1393	1391
Cooling rate [°C/min]	155.3	132.3	128.5
Time at T>1100°C [min]	6.3	6.4	6.2

Cooling rates were determined from a straight line tangential to the temperature curve at 700°C. Cooling rates in series two were higher than the cooling rate in series one. In both series one and two the highest cooling rate was found to be in the top layer and the lowest cooling rate was found to be in the bottom layer (**Table 4**). Reported cooling rates vary between 100°C/min and 300°C/min⁽¹³⁾.

Together with the differences in heating and cooling rates, another important observation is that of the different residence times above 1100°C for each layer. In both series the longest residence time above 1100°C was found to be in the middle layer, while the shortest residence time above 1100°C was found to be in the top layer. The time at temperatures higher than 1100°C for series one (1100mm H₂O) exceeded the time at temperatures higher than 1100°C for series two (1500mm H₂O). The faster downward movement of the reaction layer through the sinter bed resulted in shorter residence times above 1100°C in series two. The residence time above 1100°C is considered as very important because phase formation occurs in this temperature region⁽⁴⁾. It is assumed that the sintering process is complete when the temperature

drops below $1100^{\circ}\text{C}^{(4)}$. Therefore, the longer the residence time in this temperature region the more time there will be for phase formation. This may result in the formation of a higher content of phases that will enhance the sinter quality for example SFCA.

The airflow rate through the sinter bed is changed by changing the pressure drop over the sinter bed. The change in airflow rate through the sinter bed effects the rate of the downward movement of the combustion layer. This results in changes in the temperature-time-characteristics as described above during the sintering process.

5.3 PHYSICAL PROPERTIES

The physical properties of the sinter are characterised by the sieve analyses and the resistance to degradation by impact and abrasion at room temperature as determined with the ISO 3271 tumbler strength test. Results are shown in **APPENDIX A**.

The tumbler index (TI) is a relative measure of the resistance of the sinter to breakage by impact and abrasion. The tumbler index is expressed as the percentage of the +6.30mm fraction remaining after the tumbler test. A tumbler index greater than 70% is considered as an acceptable index for sinter. At a tumbler index greater than 70% the size degradation of the sinter by means of breakage by impact and abrasion is low and few fines will be generated.

The abrasion index (AI) is a relative measure of the size degradation of the sinter by means of abrasion. The abrasion index is expressed as the percentage of the -0.5mm fraction present after the tumbler test. An abrasion index smaller than 5% is considered as an acceptable index for sinter. At an abrasion index smaller than 5% the size degradation of the sinter by means of abrasion is low and few fines will be generated.

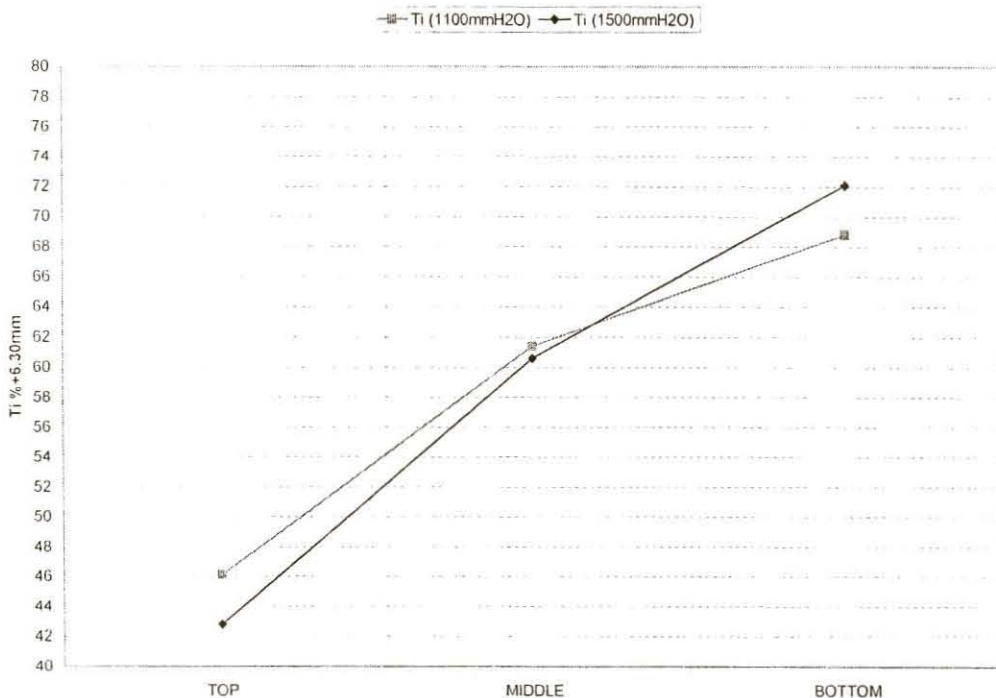
The results of the tumbler strength test are shown in **Table 5**. The abrasion index (AI) of the sinter in all the layers in both series is below 5% and is considered as an acceptable index for the sinter produced in these sinter pot tests. The results of the

tumbler test indicate that there is not a big difference between the physical properties of the sinter in the two different series (**Figure 10**). However, the results of the tumbler test imply that the physical properties of the sinter improved from the top layer to the bottom layer. Also note that the tumbler index of the sinter in the bottom layer of series one is lower than the tumbler index of the sinter in the bottom layer of series two.

Table 5: Tumbler and abrasion index of sinter produced in each layer

Parameter	Top	Middle	Bottom
Series 1: 1100mm H₂O			
TI (%+6.30mm)	46.12	61.39	68.80
TI (%-6.30+0.50mm)	49.89	34.00	26.50
AI (%-0.50mm)	3.99	4.61	4.70
Series 2: 1500mm H₂O			
TI (%+6.30mm)	42.80	60.60	72.10
TI (%-6.30+0.50mm)	53.30	35.10	23.30
AI (%-0.50mm)	3.90	4.30	4.60

Figure 10: Tumbler index of sinter produced in each layer



The results of the sieve analysis together with two important size fractions are shown in **Table 6** and are evaluated in conjunction with the tumbler index.

Table 6: Sieve analysis

Particle size mm	Series1: 1100mmH ₂ O			Series 2: 1500mmH ₂ O		
	Top	Middle	Bottom	Top	Middle	Bottom
+40	1.40	6.23	14.90	0.00	2.55	5.01
-40+25	4.66	18.97	24.20	3.27	13.00	10.49
-25+16	18.72	27.30	24.53	12.56	29.73	19.15
-16+12.5	13.33	11.98	9.15	12.41	12.90	16.78
-12.5+10	11.60	7.75	6.60	12.52	9.47	11.49
-10+5	32.88	16.49	12.11	39.64	20.92	23.23
-5	17.42	11.27	8.52	19.59	11.43	13.85
Fractions						
+16	24.78	52.50	63.63	15.83	45.28	34.65
-10	50.30	27.76	20.63	59.23	32.35	37.08
Mean size						
mm	13.75	20.25	24.17	11.82	17.57	17.05

More fines (-10mm) are produced in series two than in series one. It is also clear that the quantity of fines decreases from the top layer to the bottom layer. The quantity of the +16mm size material increases from the top layer to the bottom layer. The quantity of the +16mm size material produced in series one is higher than the quantity of the +16mm size material produced in series two (**Table 6**).

The mean particle size of the sinter in series one is also higher than the mean particle size of the sinter in series two (**Table 6**). The mean particle size increases from the top layer to the bottom layer in each series. These results indicate that the physical properties of the sinter in series one are better than the physical properties of the sinter in series two and that the physical properties improved from the top layer to the bottom layer.

Although it is not very clear from the tumbler index, it can be concluded from the sieve analysis that the physical properties of the sinter produced in series one (1100mm H₂O) are better than the physical properties of the sinter produced in series two (1500mm H₂O). The physical properties of the sinter improved from the top layer to the bottom layer as indicated by the tumbler index and sieve analysis.